

# Identified particle production in inelastic pp scattering with ATLAS

Jedrzej Biesiada for the ATLAS Collaboration

Lawrence Berkeley National Laboratory, 1 Cyclotron Road, Berkeley, CA 94720, USA

DOI: <http://dx.doi.org/10.3204/DESY-PROC-2010-01/211>

We present the observation of strange and charm hadrons using tracking information from the ATLAS Inner Detector.

## 1 Introduction

The Large Hadron Collider at CERN is designed for discovery of new physical phenomena in high- $p_T$  proton-proton collisions. However, accurate modeling of low- $p_T$  processes is critical for adequate characterization of the underlying event, which is an important background in the high- $p_T$  collisions of interest. An important ingredient in this program are identified particles containing strange and charm quarks, which can be used to tune Monte Carlo generators. Many of these particles can be identified in minimum-bias events using tracking information, and are thus important as well for evaluating tracking performance. We present here the observation of several strange and charm hadrons with the ATLAS Inner Detector [1] using a minimum-bias trigger. Data is compared with non-diffractive MC simulation, using the ATLAS MC09 tune of Pythia [2] and full GEANT4 simulation [3] of the detector. No corrections have been applied for efficiency, resolution, or other detector effects.

## 2 $K_S^0$ and $\Lambda$ decays

We reconstruct  $K_S^0$  and  $\Lambda$  decays to two charged hadrons [4] by combining pairs of tracks originating from a vertex that is well separated from the primary collision vertex. We use tracks with  $p_T > 100$  MeV and simple selections on the transverse decay length,  $L_{xy} > 4$  mm and  $L_{xy} > 30$  mm for  $K_S^0$  and  $\Lambda$  decays, respectively; and the angle between the momentum direction of the reconstructed  $K_S^0$  or  $\Lambda$  candidate and the line connecting the primary and secondary vertices,  $\cos\theta > 0.999$  and  $\cos\theta > 0.9998$  for  $K_S^0$  and  $\Lambda$  decays, respectively. Figure 1 shows the reconstructed mass distributions in approximately  $190 \mu\text{b}^{-1}$  of data; the signal and background components of the MC simulation sample are normalized separately to data. Figure 2 shows the distributions of transverse momentum and the proper decay time for  $K_S^0$  candidates, demonstrating excellent agreement between data and simulation in the proper decay time. The simulation has greater  $p_T$  on average than data; the discrepancy is under investigation.

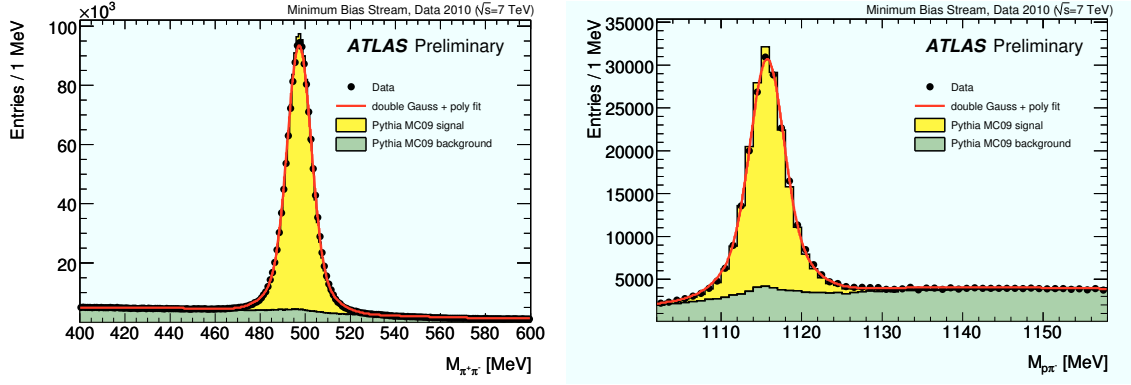


Figure 1: Comparison of measured and predicted  $K_S^0$  (left) and  $\Lambda$  (right) mass spectra in the barrel region of the Inner Detector. (Both tracks satisfy  $|\eta| < 1.2$ .) The black circles are data, while the histograms show Monte Carlo simulation (normalised to data). The solid red line is the line-shape function fitted to data.

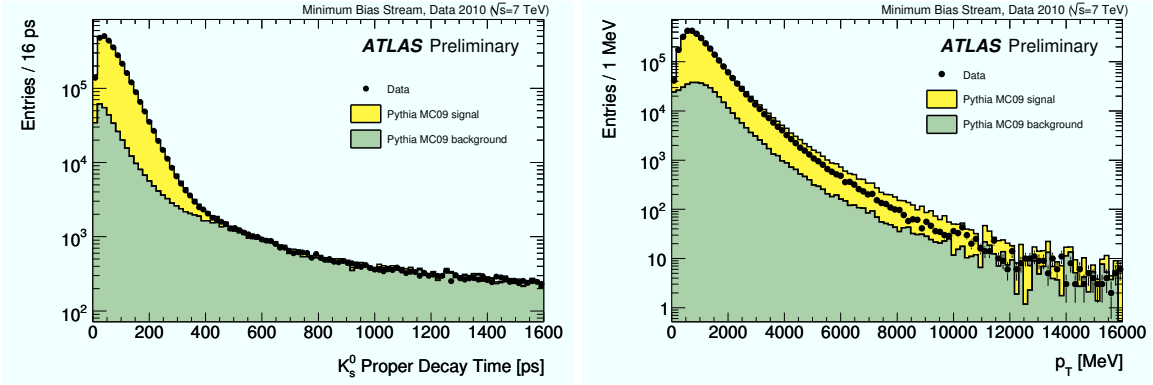


Figure 2: The proper decay time (left) and transverse momentum (right) of  $K_S^0$  candidates with reconstructed invariant mass within 20 MeV of the PDG value [5] for data and the MC sample.

### 3 Decays of $D$ mesons

We reconstruct the decay  $D^{*+} \rightarrow D^0(\rightarrow K^-\pi^+)\pi^+$  (and the charged conjugate) [6]. Since the proper decay length of the  $D^0$  meson is approximately  $123 \mu\text{m}$ , we require a positive decay length on the  $D^0$  vertex. We exploit the relatively high energy released in charm fragmentation with the selections  $p_T(D^*) > 3.5 \text{ GeV}$ ,  $p_T(K, \pi) > 1.0 \text{ GeV}$ , and  $p_T(D^*)/\Sigma E_T > 0.02$ , where  $\Sigma E_T$  is the total scalar transverse energy of the event as measured in the calorimeter and muon systems of the detector. Figure 3 shows a clear  $D^*$  peak in the distribution of the difference between the invariant mass of the  $D^*$  and the  $D^0$  candidate and a clear  $D^0$  peak in the distribution of the  $K\pi$  invariant mass, with approximately 2000 signal candidates in each peak. Figure 4 shows the reconstructed mass for roughly 1700  $D^+ \rightarrow K^-\pi^+\pi^+$  signal candidates reconstructed with similar selections, but with a tighter cut of  $L_{xy} > 1.3 \text{ mm}$  (since the  $D^+$  meson has a

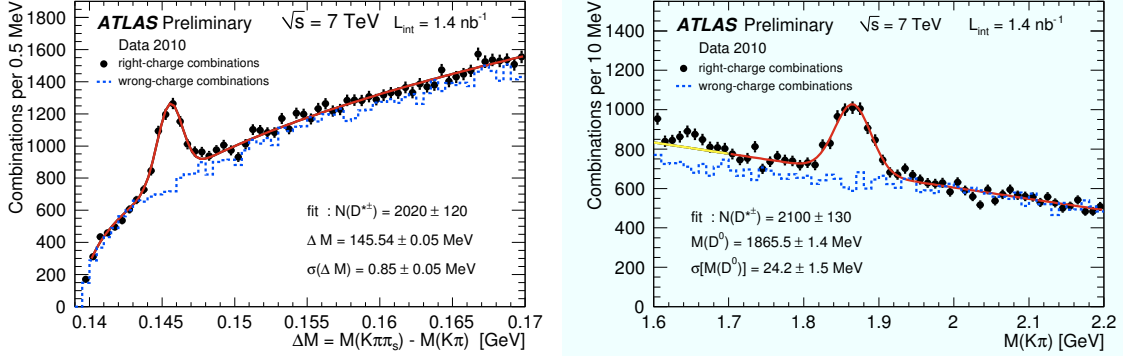


Figure 3: Left: The distribution of the mass difference,  $\Delta M = M(K\pi\pi_s) - M(K\pi)$ , for  $D^*$  candidates (points). Right: The  $M(K\pi)$  distribution for the  $D^0$  candidates in the same  $D^*$  decay mode (points). The solid curves represent fit results, while the dashed lines show the wrong-charge combinations in data.

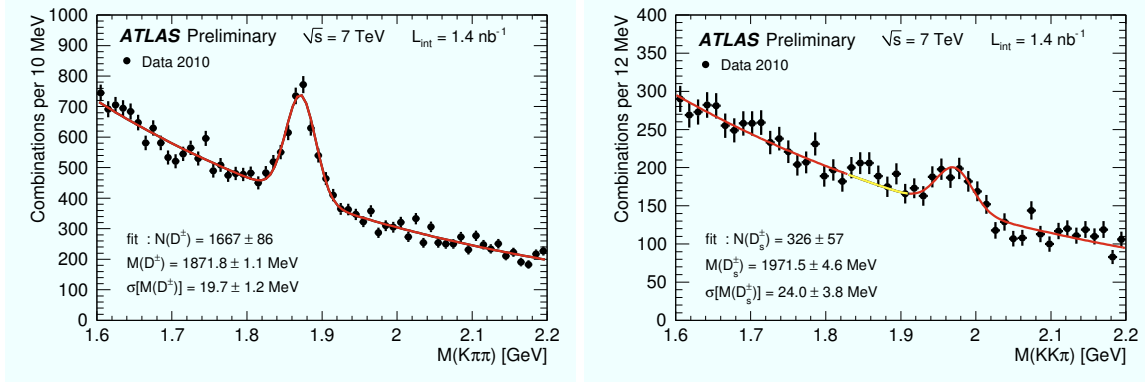


Figure 4: Left: The  $M(K\pi\pi)$  distribution for  $D^+$  candidates (points). The solid curve represents a fit to the sum of a Gaussian function and an exponential background function. Right: The  $M(KK\pi)$  distribution for  $D_s$  candidates (points).

longer lifetime) and vetos on  $D^*$  decays and  $D_s \rightarrow \Phi(K^+K^-)\pi$  reflections. Figure 4 also shows roughly 330  $D_s \rightarrow \Phi(K^+K^-)\pi$  signal candidates, reconstructed with additional cuts exploiting the vector nature of the  $\Phi$  meson and a tighter cut of  $p_T(D^*)/\Sigma E_T > 0.04$ . The fitted positions of the mass peaks are in close agreement with the PDG values [5] for these decays.

## 4 $\Xi$ and $\Omega$ Decays

We reconstruct the decays  $\Xi \rightarrow \Lambda\pi$  and  $\Omega \rightarrow \Lambda K$  [7]. As both the cascade baryon itself and the  $\Lambda$  baryon have a macroscopic proper decay length, we reconstruct the entire cascade decay chain with pointing constraints between the primary, secondary, and tertiary vertices and a

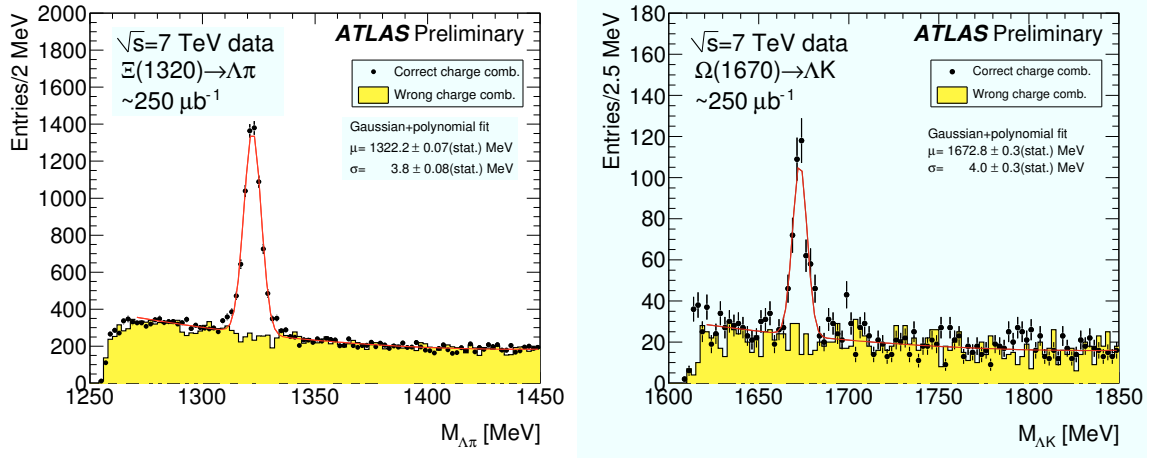


Figure 5: Left: The invariant mass of the reconstructed  $\Xi$  (left) and  $\Omega$  (right) cascade-decay candidates. The red curve shows the fit result.

mass constraint on the  $\Lambda$  candidate. For the  $\Xi$  decay, we require that the bachelor pion have a transverse impact parameter  $d_0 > 0.5$  mm and  $p_T > 150$  MeV, while for the bachelor kaon in the  $\Omega$  case we require  $d_0 > 1$  mm and  $p_T > 400$  MeV. For the  $\Xi$  baryon we require a flight distance of at least 4 mm, while for the  $\Omega$  baryon we require a flight distance of at least 6 mm,  $p_T(\Omega) > 1500$  MeV, and a veto on  $\Xi$  reflections. In both cases we require the secondary vertex to have  $\chi^2 < 7$ . Figure 5 shows the reconstructed invariant mass, showing clear signal peaks for both strange baryons, in agreement with the PDG values [5] for the mass.

## 5 Summary

We have reconstructed several hadronic decays using the ATLAS Inner Detector. The results demonstrate excellent tracking performance and accurate MC simulation.

## References

- [1] The ATLAS Collaboration, “The ATLAS Experiment at the CERN Large Hadron Collider,” JINST **3**, S08003 (2008).
- [2] The ATLAS Collaboration, “ATLAS Monte Carlo Tunes for MC09”. ATL-PHYS-PUB-2010-002.
- [3] S. Agostinelli *et al.* [GEANT4 Collaboration], “GEANT4: A simulation toolkit,” Nucl. Instrum. Meth. A **506**, 250 (2003).
- [4] The ATLAS Collaboration: “Kinematic Distributions of  $K_S^0$  and  $\Lambda$  decays in collision data at  $\sqrt{s} = 7$  TeV”. ATLAS-CONF-2010-033.
- [5] C. Amsler *et al.* [Particle Data Group], “Review of particle physics,” Phys. Lett. B **667**, 1 (2008).
- [6] The ATLAS Collaboration: “ $D^*$  mesons reconstruction in pp collisions at  $\sqrt{s} = 7$  TeV”. ATLAS-CONF-2010-034.
- [7] The ATLAS Collaboration: “Observation of  $\Xi$ ,  $\Omega$  baryons and  $K^*(890)$  meson production at  $\sqrt{s} = 7$  TeV”. ATLAS-CONF-2010-032.